Metallic surface states in elemental electrides

Ivan I. Naumov and Russell J. Hemley

Metallic surface states in elemental electrides

Ivan I. Naumov[1] and Russell J. Hemley[2]

[1]*Geophysical Laboratory, Carnegie Institution of Washington, Washington DC 20015, USA*
[2]*Department of Civil and Environmental Engineering,*
The George Washington University, Washington DC 20052, USA

Recent high-pressure studies have uncovered a new class of materials, insulating electride phases created by compression of simple metals. These exotic insulating phases develop an unusual electronic structure: the valence electrons move away from the nuclei and condense at interstitial sites thereby acquiring the role of atomic anions or even molecules. We show that they are also topological phases as they exhibit a wide diversity of metallic surface states (SSs) that are controlled by the bulk electronic structure. The electronic reconstruction occurs that involves charge transfer between the surfaces of opposite polarity making both of them metallic, resembling the appearance of the two-dimensional gas at the renowned $SrTiO_3/LaAlO_3$ interface. Remarkably, these materials thus embody seemingly disparate physical concepts – chemical electron localization, topological control of bulk-surface conductivity, and the two-dimensional electron gas. Such metallic SSs could be probed by direct electrical resistance or by standard photoemission measurements on recovery to ambient conditions.

I. INTRODUCTION

The discovery of topological insulators has inspired an interest in the systems that are insulating in the bulk but necessarily have metallic surfaces or interfaces [1,2]. Such systems can exhibit unusual or even unanticipated exotic properties. Examples include the formation of a two-dimensional electron gas at the interface between two cubic centrosymmetric insulators $LaAlO_3$ (LAO) and $SrTiO_3$ (STO). Ultimately, this phenomenon is caused by a polarization discontinuity of half of a "quantum of polarization" (or Berry phase discontinuity of π) at the interface [3-5]. Another example is insulating centrosymmetric systems with non-polar surfaces and inverted (*sp*-like) band gaps where the existence or absence of occupied SSs is decided by the Berry phase obtained by the integration across the Brillouin zone (BZ) perpendicular the surface. If the phase is π (0), then the occupied surface states (SSs) should (should not) appear within the bulk energy gap, as in the *Cmca*-4 phase of compressed hydrogen [6-10]. This criterion for the existence of SSs is in fact an extension of the classic Shockley (and later Zak) results for a simple one-dimensional model to higher dimensions [10].

Surprisingly, the above mentioned examples bear a direct relation to novel insulating forms alkali metals such as Li, Na and K called high-pressure electrides (HPEs) [11-16]. These materials are unusual with respect to their chemical bonding. On one hand, they can be viewed as pseudobinary (Na and K) or even pseudoternary (Li) ionic compounds where the "anions" or "molecules" made of valence electrons have charge of -2 [12,14-16]; on the other hand, they can be also considered as covalently bonded structures, since the insulating character arises from strong *s-p-*(*d*) multicenter hybridization [11-13,15,16]. Since the bulk band gaps in HPEs are "inverted" (the *p*-states lie lower than *s*-states), one should expect the existence of *sp*-like metallic surface (Shockley) states within the bulk band gap [17]. On the other hand, since HPEs are also ionic, a two-dimensional electron gas should appear at their polar surfaces as a result of an electronic or atomic reconstruction [3].

Here we show using Berry phase analysis that HPEs have metallic surfaces that are controlled by the topology of the bulk band structure, i.e., they are topological insulators. When a slab used to model the surface, is not symmetric and polar, then the electrons (0.5e or 1.0e per surface unit cell, depending on the formal polarization) are transferred from the valence SSs at

one surface to the conduction SSs at the opposite surface making them metallic, in close analogy with the LAO/STO system. We find that the "electronic relaxation" described above is not the only mechanism that neutralizes the polarization catastrophe and leads to metallic SSs. Another mechanism is simply to deposit one more layer either on the top or bottom of the film. Remarkably, in contrast to the usual polar systems like oxides, such a cancelation of polarity does not violates the stoichiometry of the system because the latter is composed of just *one* atomic species, effects that could been examined experimentally.

II. METHODS

Our calculations were performed using a Trouiller-Martins-type norm-conserving pseudopotential with the Perdew-Burke-Ernzerhof GGA functional as implemented in the ABINIT package [18]. A cutoff energy of 80 Ry was used for the plane-wave expansion of the valence and conduction bands wave functions. The surfaces were simulated by a system of parallel films separated by vacuum gaps. The value of a vacuum gap were chosen to be approximately equal to the thickness of the film; this is sufficient to ensure negligible wave function overlap between the replica films provided that the latter consist of 30 monolayers and more. A $16 \times 16 \times n$ Monkhorst-Pack **k**-point grid [19] was used in the surface calculations where n is the number corresponding to the surface normal; it was taken between 1 and 4, depending on the film thickness.

III. RESULTS

a. Structures

Experiments and theory show that the insulating phases of Na and K adopt a double close-packed *hP4* structure [11, 12], whereas that in Li is a *Aba2* structure [20,21]. We chose *hP4*-Na as an example (Fig. 1), but our analysis reveals that similar conclusions can be drawn for two other insulating HPEs. In the *hP4*-Na phase, the close-packed layers are stacked as *CBCACBCA…* along the z direction. The Na atoms occupy Wyckoff positions $2a$ $(0,0,0)$ and $2d$ $(2/3,1/3,1/4)$ whereas the charge density maxima are located only in layers A and B at the unoccupied $2c$ $(1/3,2/3,1/4)$ positions [11,12,15]. We assume that the surfaces of *hP4*-Na are unreconstructed; i.e., they have the smallest possible surface primitive unit cell consistent with

the bulk symmetry In principle, a noticeable degree of covalency in the bonding may allow surface reconstruction. To check this possibility, we examined possible (2×2) and (3×3) reconstructions on the (0001) surface allowing the atoms to move parallel to the surface (such a constrain makes it possible to keep the applied pressure of ~200 GPa practically unchanged). We introduced different initial (2×2) and (3×3) surface distortions and found that the system always relaxed to the unreconstructed (1×1) structure.

We start with the question as to which surfaces of a model electride system are polar. In accordance with the definition of Ref. [5], polar surfaces are those for which $\mathbf{P}_{\text{bulk}} \cdot \mathbf{n} \neq 0$, where $\mathbf{P}_{\text{bulk}}$ is the bulk polarization and $\mathbf{n}$ is the normal to the surface plane. It is important that $\mathbf{P}_{\text{bulk}}$ is a multivalued (formal) quantity and therefore captures not only the difference between the surfaces of distinct orientations, but also between the different terminations for a given orientation: different terminations correspond to different choices of the bulk ionic basis [5].

To find the lattice of allowed values $\mathbf{P}_{\text{bulk}}$ in *hP4*-Na consider first the standard choice of the primitive ionic basis within which the Na atoms occupy the following 4 positions: (0,0,0), (0,0,1/2), (2/3,1/3,1/4) and (1/3,2/3,3/4); this basis corresponds to the yellow parallelogram in Fig. 2b. For this choice, the calculated total (electronic + ionic) Berry phases along the shortest reciprocal lattice vectors $\mathbf{G}_1$, $\mathbf{G}_2$, and $\mathbf{G}_3$ were found to be π, π, and $-\pi/2$, respectively; all the phases are subject to addition of any integer multiple of 2π. This means that the lattice sought is centered in e/Ω ($\boldsymbol{a}_1$, $\boldsymbol{a}_2$,$-\boldsymbol{c}/2$), where Ω is the volume of a primitive unit cell, $\boldsymbol{a}_1$, $\boldsymbol{a}_2$, $\boldsymbol{c}$ are the primitive translations vectors of the *dhcp* structure. The difference between two arbitrary values of $\mathbf{P}_{\text{bulk}}$ is 2e$\mathbf{R}$/Ω, where $\mathbf{R}$ is a lattice vector, and the factor 2 appears due to the fact that our system is a spin-degenerate insulator [28]. The resulting lattice $\mathbf{P}_{\text{bulk}}$ is in fact only a sublattice of the complete polarization lattice.

To identify the latter we need to try other possible choices of a 4-atom unit cell. One possibility is to move the first Na atom in the standard unit cell from the position (0,0,0) to (0,0,1) on condition that all the other atoms are fixed. Upon such a moving the total Berry phases along $\mathbf{G}_1$, $\mathbf{G}_2$, and $\mathbf{G}_3$ become π, π, and $+\pi/2$. This generates another polarization sublattice: e/Ω ($\boldsymbol{a}_1$, $\boldsymbol{a}_2$, $\boldsymbol{c}/2$) modulo 2e$\mathbf{R}$/Ω. One more modification of the standard unit cell basis can be achieved by shifting all the primitive translations $\boldsymbol{a}_1$, $\boldsymbol{a}_2$ and $\boldsymbol{c}$ by a vector $(\boldsymbol{a}_1 + \boldsymbol{a}_2)/2$ relative to the crystal. This shift changes the positions of atoms within the unit cell, now they are

(1/2,1/2,0), (1/2,1/2,1/2), (1/6,5/6,1/4) and (5/6,1/6,3/4); this basis is shown by green rectangle and parallelogram in Fig. 2. Correspondingly, the total Berry phases become 0, 0, and $-\pi/2$, respectively, whereas the origin of the polarization lattice $\mathbf{P}_{\text{bulk}}$ shifts to e/Ω (0, 0, $-c$/2). When combined, all the three found sublattices organize the sought complete lattice, which is e/Ω (0,0, c/2) modulo e$\mathbf{R}$/Ω (but not 2e$\mathbf{R}$/Ω).

Since the center of the complete polarization lattice $\mathbf{P}_{\text{bulk}}$ is shifted along the z axis, it is clear that the low-index plane (0001) (or (000$\bar{1}$)) is polar: for this plane the relation $\mathbf{P}_{\text{bulk}} \cdot \mathbf{n} \neq 0$ is satisfied [5]. The polar character of the plane can be easily visualized (Fig. 2). The Wannier functions (WFs) in *hP4*-Na are centered exactly on the 2c Wyckoff positions [15]; thus, they share the same z-planes with the ions A and B, but not C. As each WF carries a -2 charge, the A and B layers have a total charge of -1 whereas the C layers are +1 per two-dimensional unit cell. With such charges, the stacking sequence $CBCA...CBCA$ can be viewed as a sequence of alternatively charged layers +1 -1 +1 -1...+1 -1 +1 -1 (Fig. 2a). In contrast to (0001), the plane (10$\bar{1}$ 0) (or ($\bar{1}$010)) can be both polar and non-polar depending on termination. The polar surface corresponds to $\mathbf{P}_{\text{bulk}}$ = e/Ω (a_1, a_2, $-c$/2) or to a 4-atom primitive unit cell that carries a dipole moment (shown in yellow in Fig. 2b). When this unit cell is stacked along the direction perpendicular to the (10$\bar{1}$ 0) plane, the layers become charged as +2 -1 -1... +2 -1 -1. The non-polar surface corresponds to $\mathbf{P}_{\text{bulk}}$ = e/Ω (0, 0, $-c$/2) or to the primitive unit cell shown in green in Fig. 2b. The latter has no dipole moment, and when is stacked perpendicular to (10$\bar{1}$ 0) plane, the layers become charged as -1+2 -1 ... -1+2 -1.

b. (0001) Polar Surface

The calculated surface electronic structure for the 8-unit-cell thick film that models the polar (0001) surfaces is shown in Fig. 3a; the calculations for thicker slabs lead to only slightly different quantitative results. One can see that the slab is metallic: two bands indicated by thick black curves cross the Fermi level (E$_F$). These two bands are nothing but Shockley SSs: they form inside the bulk "inverted" energy gap. One of them falls out of the allowed bulk valence band and the other from the allowed conduction band. Our analysis shows that the first one is localized on the surface where the top layer is A and contains approximately 1.5e, whereas the second is confined to the opposite "C-surface" and contains approximately 0.5e. This arises from

half an electron being transferred from one side of the slab to another upon "cutting" it out from the bulk. This is exactly the charge needed to screen the electric field that would exist inside the slab if no relaxation processes were allowed. In other words, the appearance of free charges $\pm 0.5e$ (per surface unit cell) on the opposite side compensates the polarization surface charges completely and makes the slab electrostatically stable. The fact that electrons move from A- to C-surface is quite natural because the A layers in the bulk are charged as -1 whereas the C layers as $+1$. Thus, the metallization of polar surfaces $hP4$-Na can be viewed as a result of "electrostatic" doping, as in the case of the polar LAO/STO interface [4]. In our case, however, the metallization is associated with the SSs rather than with the local bending of the bulk-like states both in the LAO and STO components.

We stress that although both $hP4$-Na and the LAO/STO system exhibit surface metallization due to "electronic reconstruction" in which the electrons move between opposite surfaces, the mechanisms of these reconstructions differ. In LAO/STO, the conduction and valence bands preserve their respective identities and the charge transfer is caused by their local bending when the film exceeds some critical thickness [3,5,22]. In contrast, in HPEs the charge transfer takes place between the SSs that appear due to Shockley-inverted bulk energy gaps (no SSs exist on polar surfaces of LaAlO₃). The existence of SSs near the E_F greatly facilitates the electronic transfer between the surfaces, and such a transfer (~0.44e) is already realized in the 1-unit-cell thick film. We emphasize that the charge transfer between the surfaces should not be understood literally as involving only the very top and very bottom surface layers. The actual spread of the SSs into the bulk region is 2-3 lattice parameters (Fig. 4), and the spatial confinement of the free electrons near the surfaces is of the same order.

For the polar (0001) surfaces considered above, the slabs were built by stacking the bulk primitive units cells or $CBCA$ blocks along the z–direction. It is easy to see that the polarity of such surfaces can be simply cancelled by adding one more layer on the top or bottom of the slab. When one more C layer is placed on the top, the slab becomes organized as $CBCA…CBCA\textbf{C,}$ thereby acquiring the inversion centre ($\mathbf{r} \rightarrow -\mathbf{r}$); the new layer is highlighted in bold. On the other hand, if an additional A layer is deposited on the bottom, the structure becomes $\textbf{A}CBCA…CBCA$; it contains a mirror symmetry plane ($z \rightarrow -z$). In both cases, the slabs should be metallic as they

now contain an odd layers or electrons, namely $4n+1$, where n is the number of complete bulk unit cells.

c. (0001) Nonpolar and other surfaces

We now consider the band structure of a 33-layer ($n=8$) slab with an inversion center (Fig. 3b). On can see doubly degenerate Shockley SSs, which our analysis shows are localized both at the top and bottom surfaces. Since both the SSs fall out of the allowed bulk conduction bands and are degenerate, together they contain exactly 1 electron or a half of electron each. Such a low population may intuitively be understood by the fact that now both the surfaces are of C type or the surfaces with +1 termination. In going to the slabs with a mirror plane the situation changes dramatically, both the SSs fall out of the allowed bulk valence bands (Fig. 3c). Together they contain exactly 3 electrons or 1.5 electrons each. Again, this result can be anticipated: now both the surfaces are of A type with −1 termination.

In Fig. 3 we considered only the slabs with terminations $C...A$, $C...C$, and $A...A$; all the other possible terminations lead to similar surface bands in terms of their fillings and character (in the limit of infinite thickness). In fact, all the combinations of terminations can be broken up into three groups: (i) (+1...−1), (ii) (+1...+1) and (iii) (−1...−1). They lead to three different families of 2-branched surface bands with fractional fillings ¼+¾, ¼+¼ and ¾+¾, correspondingly. The typical valence charge densities corresponding to these families are presented in Fig. 5.

It may appear that the SSs on one surface are affected by the opposite surface, at least for the polar slabs (−1...+1). This, however, is not the case if the polarity is completely canceled. When the electric field inside the slab is indeed zero, then the SSs are entirely defined by a given termination, whether it is −1 or +1. This is the reason why the dispersion curves of the SSs corresponding to the same termination, say +1, are almost identical and practically not altered by the opposite surface (Fig. 3). This observation leads to the interesting conclusion that the fillings of the SSs in *both* polar and non-polar (0001) slabs can be predicted by knowing the corresponding bulk Berry phase alone. Intuitively, the fractional fillings of the SSs in the non-polar slabs with −1...−1 (*n*-type) and +1...+1 (*p*-type) terminations could be anticipated even without involving Berry phase arguments. Indeed, the *n(p)*-type terminations can be considered

as $n(p)$-doped with a charge density of $\pm 0.5e$ (e is negative) per unit cell area. To this end, the SSs on the n-type terminations should fall out of the bulk conduction band and be ¼ filled, whereas on the p-type of the bulk valence band and be ¾ filled.

We now proceed to the discussion of $(10\bar{1}0)$-type surfaces. We first consider polar surfaces, which can be constructed by stacking of the 4-atom bulk unit cells with a dipole moment (shown in yellow in Fig. 2b). In practice, such a stacking is more convenient to perform by using a "double" cell with the orthogonal primitive vectors $2a_1 + a_2$, a_2 and c (also shown in yellow in Fig. 2b): the vector $2a_1 + a_2$ is normal to the $(10\bar{1}0)$ plane. The calculated surface band structure for a 24-layer-thick slab with such polar surfaces is presented in Fig. 6a. As in the polar (0001) case, the slab is characterized by two metallic surface states that fall out of the conduction and valence bulk bands and form on the opposite surfaces. Now, however, a charge transfer of $1e$ per surface unit cell area should be transferred between the surfaces to screen the macroscopic electric field inside the film. Indeed, intuitively we may regard each pair of two neighboring −1 layers in bulk as being half compensated from each of their two immediate +2 neighbors. At the surface, however, the pair is only half compensated, because it has only a single +2 neighbor. Direct calculations show that each SS band indeed contains approximately 1 electron.

The polarity of a $(10\bar{1}0)$-type surface can be cancelled by introducing an additional layer containing C atoms (Fig. 2b). This modification substitutes a +2…−1−1 slab for a +2…+2 one with an inversion center, which gives two +2 terminations, instead of one such termination in the polar slab, and the two SSs become degenerate (Fig. 6b). Naturally, together they contain 2 electrons or 1 electron each. As previously mentioned, the $(10\bar{1}0)$ slabs with −1…−1 terminations also have non-polar surfaces. Such slabs can be built from the 4-atom bulk unit cells, which are symmetrical (shown in green in Fig. 2b). Since for this bulk unit cell the Berry phase across the BZ perpendicular to this surface is 0, we should not expect the existence of any metallic SSs on them [6-9]. This is true when the slabs exceed some critical thickness. Otherwise they are surface semi-metals rather than insulators, as in the case of a 24-layer-thick slab (Fig. 6c). For this slab, we see that indeed there is no *direct* overlap between the valence and conduction surface bands. However, the bottom of the conduction band at the $\bar{Z}$ point drops below the top of the valence band at the $\bar{X}$ and $\bar{M}$ points. As the thickness increases, the indirect overlap between the bands decreases and the slab gradually turns into an insulator. It is

interesting to note that for the −1…−1 slabs both the valence and conduction SSs are doubly degenerate due to the inversion symmetry (Fig. 6c).

III. DISCUSSION

All polar surfaces apparently discussed in the literature to date are those of either ionic oxides or covalent semiconductors like ZnS or GaAs [23,24]. Here we find unusual polar surfaces that are realized in materials composed of just *one* atomic species. The principal difference between HPEs and polar compounds is that in the latter the polarity cannot be "compositionally" canceled without stoichiometry violation. By contrast, in HPEs such a cancellation can be easily achieved by the addition of a new layer that preserves the unary character of the system. The layer makes the slab more symmetric and leads to doubly degenerate metallic SSs. Another important difference between the HPEs and multi-component compounds is that in the former the "compositional" charge cancellation (adding a new layer) leads to the same SSs as the "electronic reconstruction" that involves a charge transfer between the opposite surfaces, provided that the resulting surface/termination is the same. As a result, the fillings of the SSs for the both scenarios of reconstructions can be predicted from the analysis of bulk Berry phases.

The appearance of metallic SSs in high-pressure forms of alkali metals is also interesting because these metals do not exhibit any occupied SSs at ambient conditions: the band gaps in them lie above the E_F [25]. We showed, however, that such SSs do exist in the insulating HPEs, where the E_F is within the global band gap. Though here we consider only non-conducting Na, other insulating HPEs – i.e., K and Li − share similar behavior. K in its electride phase has the same structure as *hP4*-Na and therefore should exhibit similar properties. In contrast, Li adopts a more complicated non-centrosymmetric HPE structure (*Aba2*) with 20 atoms per primitive unit cell. We calculated the polarization lattice in *Aba2*-Li and found it to be $P_{bulk} = e/\Omega$ (a, −0.14b, −0.14c) modulo $2e\mathbf{R}/\Omega$. Clearly, a (100) surface, for example, is polar and should behave in much the same way as (0001) counterpart in *hP4*-Na. We expect that its electronic relaxation will involve Shockley-type SSs making them metallic. Anisotropy of the work function is also expected [26]. At ambient conditions, *bcc*-Na exhibits a weak anisotropy of the work function, which increases with the surface packing density in going from the (111) surface to (100) and (110) (2.79, 2.80, 3.00 eV, respectively [26]). It is clear that the anisotropy of the work function

in *hP4*-Na should be much more pronounced. Indeed, due to strong *sp*-hybridization in *hP4*-Na, the directional character of *p*-orbitals should come into play in this phase. As a result, the work function should strongly depend on whether the *p*-states are oriented parallel or perpendicular to the surface. This question calls for further investigation.

In our analysis above we have tacitly assumed that the macroscopic material is congruent to a film which exposes the surfaces to vacuum. In reality, however, the electrides considered here so far have only been observed under pressure; thus the phases are always surrounded by some other material producing external the pressure. Our main conclusion with respect to the appearance of two-dimensional metallicity, however, is still holds whenever the second material is a dielectric that lacks polar surfaces, e.g., a clean diamond surface used in a diamond-anvil cell experiment. For the latter, we can assume the electride material with the geometry of a thin film is sandwiched between two diamond-like sheets, so that it has two interfaces rather than two surfaces. It is clear, however, that in going from the surfaces to interfaces the polar discontinuities, $(\mathbf{P}_1 - \mathbf{P}_2) \cdot \boldsymbol{n}$ (if any) will not change if open-circuit boundary conditions are assumed (the electric field is zero within both the sheets) [27]. The field will be confined only to the electride interior, like in a capacitor, due to equal but opposite charges on the interfaces. To avoid the "polarization catastrophe", this field will be compensated by a charge transfer between the SSs, making them metallic as in the case of electride-vacuum interfaces discussed above.

In addition to Li, Na and K, other simple metals that also develop valence electron localization but become "almost insulating" under compression, e.g., Mg [28], Ca [15,29] and Al [30]. Our main findings, however, are not applicable to them because they do not open a global band gap and therefore do not have polar surfaces that would lead to metallic SSs associated with the cancellation of polarity. Of course, these metals can still form metallic SSs within the bulk band gap. In Mg and Al such states are likely to be Shockley-type as these metals have well pronounced *sp*-inverted band gaps [17]. They therefore can be predicted from the bulk band structure either by inspecting the character of the band gap [17] or by analyzing the corresponding Zak's phase $Z(\mathbf{k})$ [10]. The situation differs for Ca due to the admixture of *d*-states that quench the appearance of Shockley SSs [17, 31]. This is the reason why no direct connection was found between $Z(\mathbf{k})$ and existence of SSs in *fcc* Ca at 7.5 GPa, despite the fact that the system represents a topological semimetal.

In summary, we show that the recently discovered insulating HPE phases of simple elemental materials exhibit a diversity of metallic SSs that can be predicted from the bulk electronic structure due to a specific *bulk-surface* correspondence. Such a correspondence can be understood within the modern theory of polarization in terms of a Berry phase approach. We predict that the Shockley-type SSs with fractional fillings appear on their polar surfaces due to electronic and atomic reconstruction. Electronic reconstruction involves a charge transfer between the surfaces of opposite polarity making both of them metallic as in other two-dimensional electron gas systems. The SSs considered could be probed *in situ* at high pressure using resonant inelastic x-ray scattering experiments or by standard photoemission measurements if the materials can be recovered to ambient pressures.

Acknowledgements

References

1. M. Z. Hasan and C.L. Kane, Rev. Mod. Phys. **82**, 3045 (2010).

2. X.-L. Qi and S.-C. Zhang, Rev. Mod. Phys. **83**, 1057 (2011).

3. N. C. Bristowe, P. Ghosez, P. B. Littlewood, and E. Artacho, J. Phys: Condens. Matter **26**, 143201 (2014).

4. M. Stengel, Phys. Rev. Lett. **106**, 136803 (2011).

5. M. Stengel, Phys. Rev. B **84**, 205432 (2011).

6. A. A. Burkov, M. D. Hook, and L. Balents, Phys. Rev. B **84**, 235126 (2011).

7. P. Delplace, D. Ullmo and G. Montambaux, Phys. Rev. B **84**, 195452 (2011).

8. T. Kariyado and Y. Hatsugai, Phys. Rev. B **90**, 085132 (2014).

9. R. Takahashi and S. Murakami, Phys. Rev. B **88**, 235303 (2013).

10. I. I. Naumov and R. J. Hemley, Phys. Rev. Lett. **117**, 206403 (2016).

11. Y. Ma, M. Eremets, A. P. Oganov, Y. Xie, I. Trojan, S. Medvedev, A. O. Lyakhov, M. Valle, and V. Prakapenka, Nature **458**, 182 (2009).

12. M. Marque´s, G. J. Ackland, L. F. Lundegaard, G. Stinton, R. J. Nelmes, and M. I. McMahon, Phys. Rev. Lett. **103**, 115501 (2009).

13. T. Matsuoka and K. Shimizu, Nature **458**, 186 (2009).

14. M.-S. Miao and R. Hoffmann, Acc. Chem. Res. **47**, 1311 (2014).

15. I. I. Naumov and R. J. Hemley, Phys. Rev. Lett. **114**, 156403 (2015).

16. M.-S. Miao, R. Hoffmann, J. Botana, I. I. Naumov, and R. J. Hemley, Angew. Chem. Int. Ed., **56**, 972 (2016).

17. F. Schiller and C. Laubschat, Phys. Rev. B **74**, 085109 (2006).

18. X. Gonze, B. Amadon, P.M. Anglade, J.-M. Beuken, F. Bottin, P. Boulanger et al., Comp. Phys. Comm. **180,** 2582 (2009).

19. H. J. Monkhorst and J. D. Pack, Phys. Rev. B **13**, 5188 (1976).

20. M. Marques, M. I. McMahon, E. Gregoryanz, M. Hanfland, C. L. Guillaume, C. J. Pickard, G. J. Ackland, and R. J. Nelmes, Phys. Rev. Lett. **106**, 095502 (2011).

21. J. Lv, Y. Wang, L. Zhu, and Y. Ma, Phys. Rev. Lett. **106**, 015503 (2011).

22. J. Lee and A. A. Demkov, Phys. Rev. B **78**, 193104 (2008).

23. C. Noguera, J. Phys: Condens Matter, **12**, R367 (2000).

24. P. W. Tasker, J. Phys C: Solid State Phys. **12**, 4977 (1979).

25. L. Kleinman, Phys Rev B **6**, 1142 (1972).

26. C. J. Fall, N. Binggeli, and A. Baldereschi, Phys. Rev. B **58**, R7544 (1998).

27. D. Vanderbilt and R. D. King-Smith, Phys. Rev. B **48**, 4442 (1993).

28. P. Li, G. Gao, Y. Wang, and Y. Ma, J. Phys. Chem. C **114, 2**1745 (2010).

29. M. Hirayama, R. Okugawa,T. Miyake, and S. Murakami, Nature Commun. **8***,* 14022 (2017).

30. C. J. Pickard and R. J. Needs, Nature Materials **9**, 624 (2010).

31. W. A. Harrison, Physica Scripta **67**, 253 (2003).
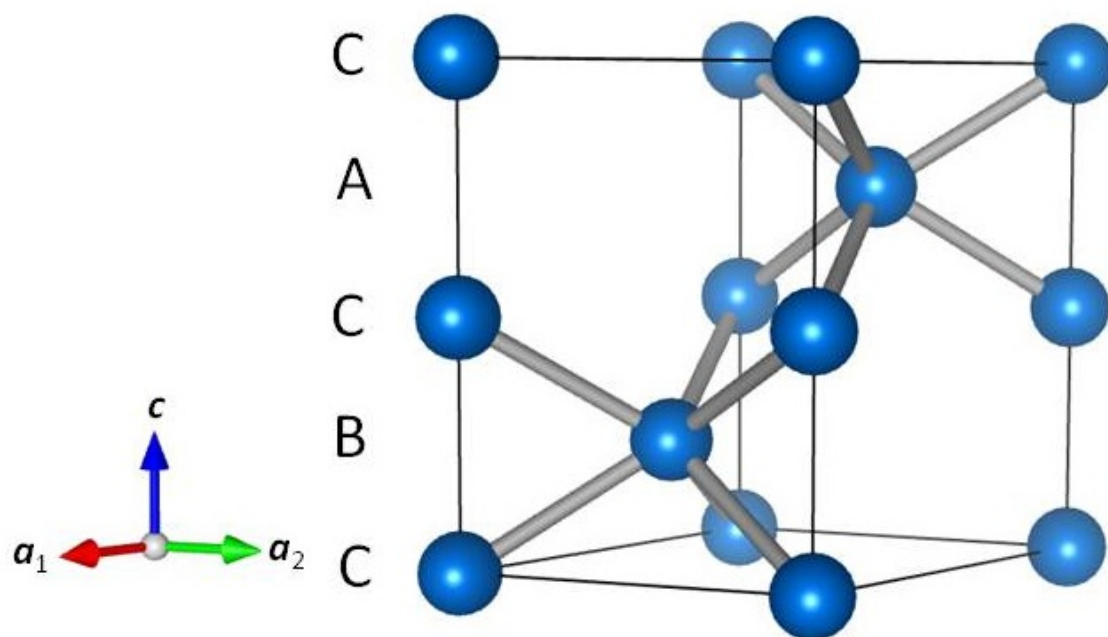
Figure 1. Primitive unit cells of *hP4*–Na (space group *P6₃/mmc*). In this structure the close-packed layers are stacked in *CBCACBCA*... fashion along the **c** axis.
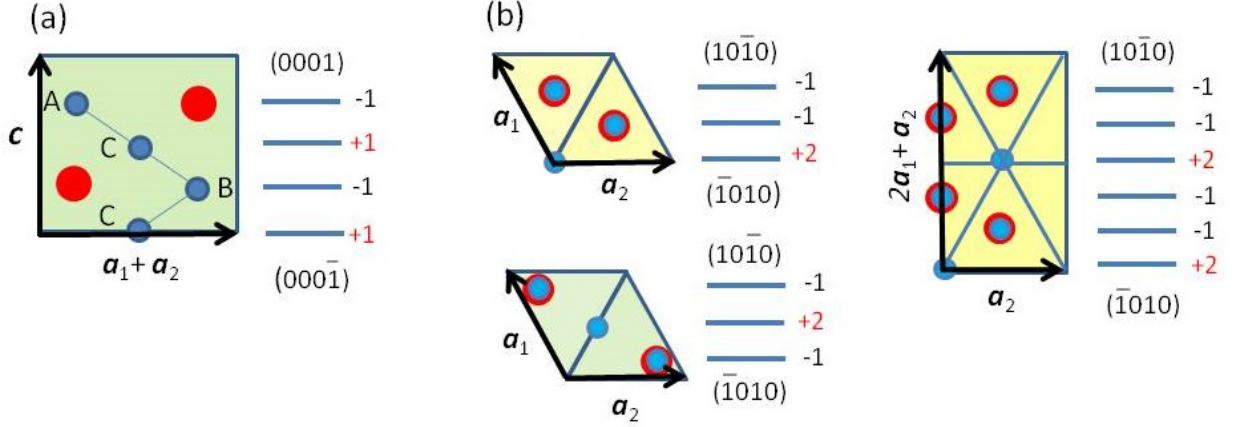
Figure 2. Ionic basis corresponding to polar and non-polar *hP4*-Na surfaces described in the text. Blue and circles indicate Na atoms and WF centers, respectively. (a) (0001) surface. The positions of atoms and WF centers are shown in the $(2\bar{1}\bar{1}0)$ plane (Miller-Bravias indices are used). The green rectangle outlines the atoms belonging to a bulk unit cell. When this unit cell is stacked along the *z*–direction, a (0001) polar surface is created. (b) $(10\bar{1}0)$ surface. Shown are the positions of atoms and WF centers projected on the (0001) plane. The yellow parallelogram indicates a standard choice of unit cell. When this cell (or the "doubled" cell depicted as yellow rectangular) is stacked along the direction normal to the $(10\bar{1}0)$ surface, a polar surface appears. A new unit cell can be obtained from the standard one by shifting both the primitive vectors, a_1 and a_2, by $(a_1 + a_2)/2$ (shown in green, it is also presented in panel (a)). When stacked in the same way, it leads to a $(10\bar{1}0)$ non-polar surface.
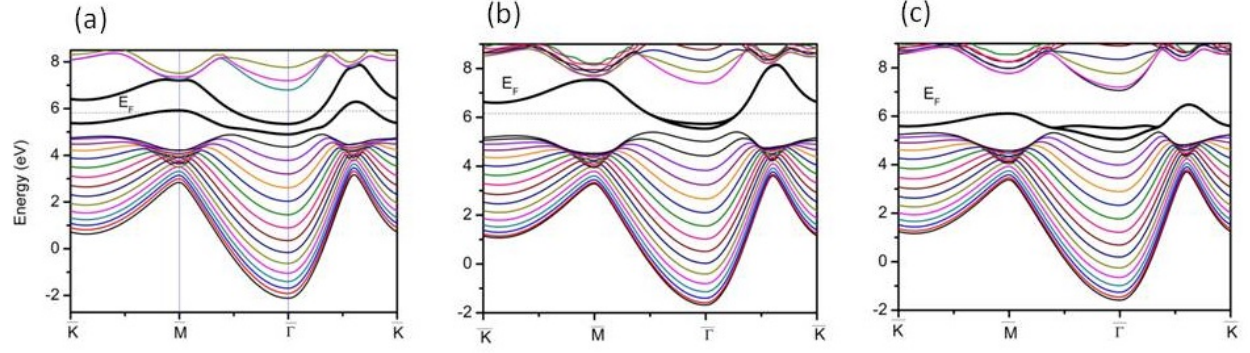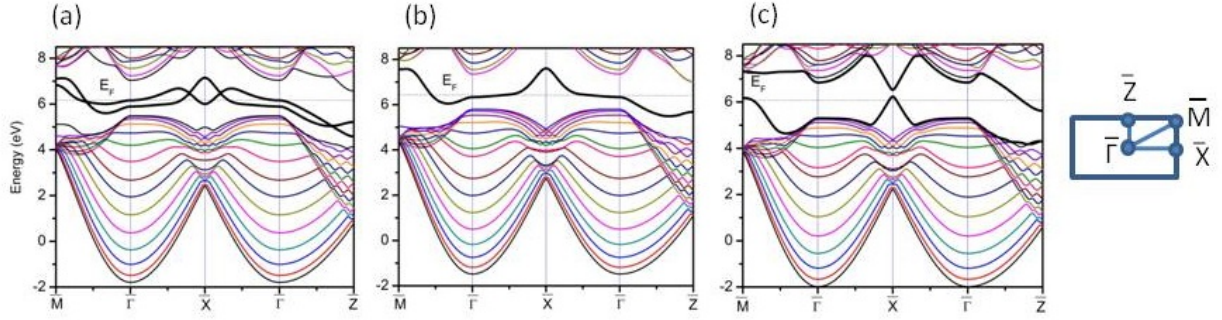
Figure 3. Two-dimensional energy bands of different *hP4*-Na slabs whose boundaries are (0001) surfaces. The surface states are indicated by thick black curves that cross the E_F. (a) 8-unit-cell thick slab (32 layers or 32 atoms per supercell). The slab is built by stacking of bulk primitive unit cells (shown in yellow in Fig. 2) along the **c** direction. (b) 8.25-unit-cell thick slab (33 layers) with an additional C layer that induces an inversion center. (c) 8.25-unit-cell thick slab with an additional A layer that induces a mirror plane. In cases (b) and (c), the SSs become degenerate as the slab becomes infinitely thick.
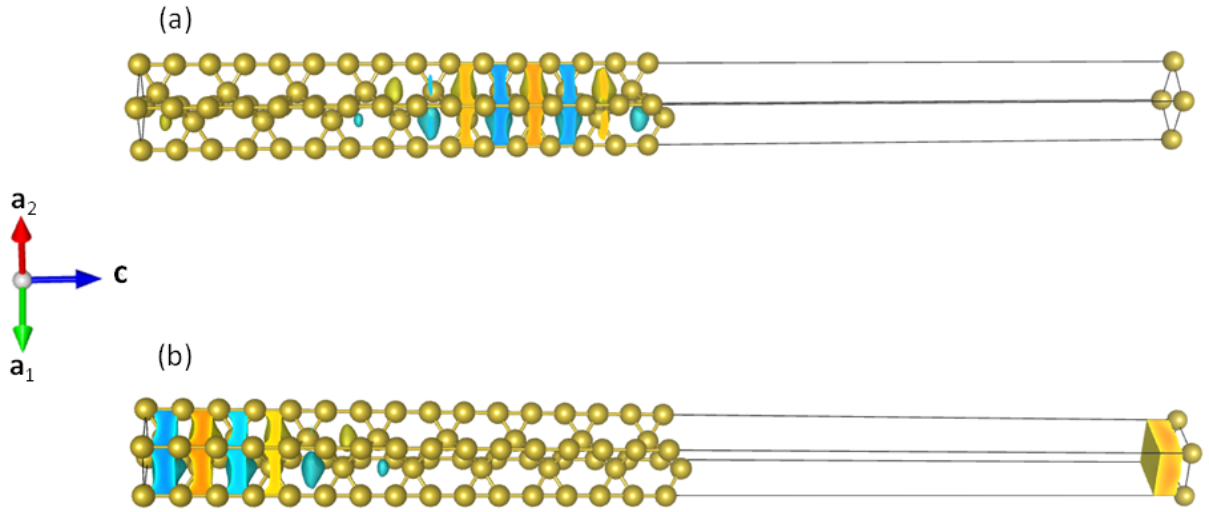
Figure 4. Surface band wave functions at Γ that correspond to 8-unit-cell thick slab with polar surfaces (Fig. 3a). (a) for the lower (in energy) surface state and (b) for the upper surface state. Isocontours (at ±2.0) are shown within a supercell containing both the atoms and vacuum gaps. One can see that the SSs are localized in the 2-3 bulk unit cells adjacent to the corresponding surface.
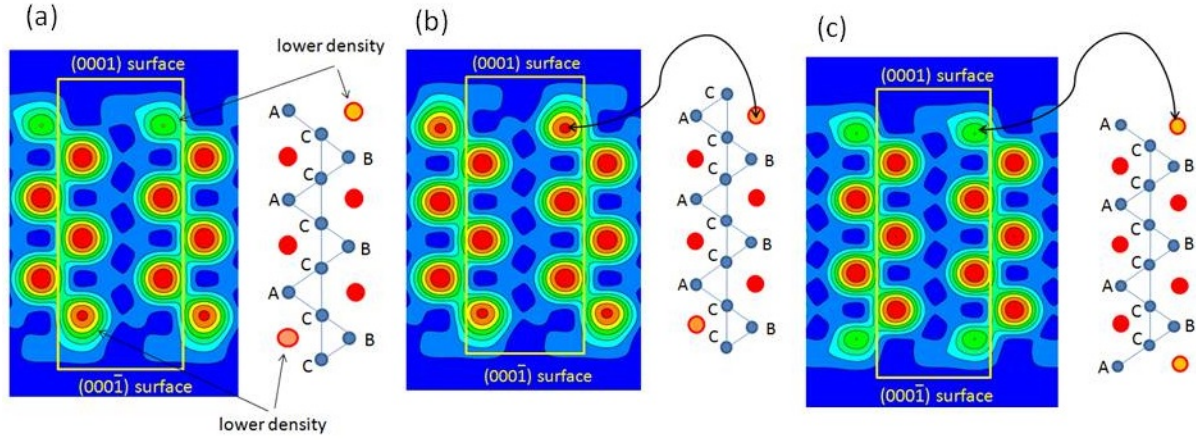
Figure 5. The valence charge densities that correspond to Fig. 3, but calculated for thinner slabs. The density increases as the color changes from blue to red. (a) a 3-unit-cell slab with terminations $C…A$ or $+1…-1$, (b) a 3.25-unit-cell slab with terminations $C…C$ or $+1…+1$, and (c) a 3.25-unit-cell slab with terminations $A…A$ or $-1…-1$. For each case, the yellow lines encircle the atoms belonging to a surface supercell; the latter is also schematically shown on the right side of the picture. One can see that the charge density associated with the A or -1 surface layers is lower than that in the bulk. This is connected with the fact that their SSs are only ¾ -filled. At the same time the charge density associated with the C (+1) surfaces are slightly higher than that in the bulk. The additional density electronic charge from their SSs that are quarter–filled .

Figure 6. Two-dimensional energy bands of different Na-*hP4* slabs whose boundaries are $(10\bar{1}0)$ surfaces. The SSs that cross the E_F are indicated by thick black curves. (a) 24-layer-thick slab (32 atoms per supercell) which is organized from the bulk primitive unit cells shown in yellow in Fig. 2b. (b) 25-layer-thick slab (34 atoms/supercell). It is obtained from (a) by adding a new layer consisting of C atoms. This new layer makes the slab centrosymmetric. (c) 24-layer-thick centrosymmetric slab (32 atoms/supercell) which is built from the bulk primitive unit cells shown in green in Fig. 2.